

# In Situ Investigation of Leaf Water Status by Portable Unilateral Nuclear Magnetic Resonance<sup>1,2</sup>[C][W][OA]

Donatella Capitani, Federico Brilli, Luisa Mannina, Noemi Proietti, and Francesco Loreto\*

Consiglio Nazionale delle Ricerche-Istituto di Metodologie Chimiche (D.C., L.M., N.P.) and Istituto di Biologia Agroambientale e Forestale (F.B., F.L.), 00015 Rome, Italy; and Dipartimento di Scienze e Tecnologie Agroalimentari Ambientali e Microbiologiche, Università degli Studi del Molise, 86100 Campobasso, Italy (L.M.)

A portable unilateral nuclear magnetic resonance (NMR) instrument was used to detect in field conditions the water status of leaves of herbaceous crops (*Zea mays*, *Phaseolus vulgaris*), mesophyllous trees (*Populus nigra*), and natural Mediterranean vegetation characterized by water-spending shrubs (*Cistus incanus*) and water-saving sclerophyllous trees (*Quercus ilex*). A good relationship was observed between NMR signal, leaf relative water content, and leaf transpiration in herbaceous leaves undergoing fast dehydration or slowly developing a drought stress. A relationship was also observed between NMR signal and water potential of *Populus* leaves during the development of a water stress and when leaves recovered from the stress. In the natural vegetation, the relationship between NMR signal and water status was found in *Cistus*, the species characterized by high transpiration rates, when measured during a drought stress period and after a rainfall. In the case of the sclerophyllous *Quercus*, the NMR signal, the relative water content, and the transpiration rate did not change at different leaf water status, possibly because a large amount of water is compartmentalized in cellular structures and macromolecules. The good association between NMR signal and relative water content was lost in leaves exposed for 24 h to dehydration or to an osmotic stress caused by polyethylene glycol feeding. At this time, the transverse relaxation time became longer than in leaves maintained under optimal water conditions, and two indicators of membrane damage, the ion leakage and the emission of products of membrane lipoxygenation [(Z)-3-hexenal, (Z)-3-hexenol, and (E)-2-hexenol], increased. These results taken all together give information on the physiological state of a leaf under a developing stress and show the usefulness of the NMR instrumentation for screening vegetation health and fitness in natural and cultivated conditions. It is concluded that the portable unilateral NMR instrument may be usefully employed in field conditions to monitor nondestructively the water status of plants and to assist agricultural practices, such as irrigation scheduling, to minimize stomatal closure and the consequent limitation to plant production.

The application of in vivo NMR to plants and plant tissues has brought significant contributions across a wide range of topics, reviewed by Ratcliffe and Shachar-Hill (2001) and Verpoorte et al. (2007). High-field magnets have been used to perform techniques, such as magnetic resonance imaging and magnetic resonance microscopy (Bottomley et al., 1986; Scheenen et al., 2000; Van As, 2007), that provided an integrated view of the topological distribution of water in plant tissues such as seeds (Manz et al., 2005), stems (Van As, 2007), and leaves (Veres et al., 1993). These techniques may also help to detect water movement through xylem vessels (Van As, 2007) and may reveal a contribution of

bound water consequent to membrane injury (Maheswari et al., 1999) or changes of membrane permeability during osmotic stresses (van der Weerd et al., 2002).

Low-field proton NMR relaxometry is a particularly important tool to investigate plant water relations as well as water compartment, diffusion, and movement, since it detects protons predominantly contributed by <sup>1</sup>H<sub>2</sub>O contained in plant tissues. This technique allows the proton spin density, the NMR signal, the longitudinal relaxation time (T<sub>1</sub>), and the transverse relaxation time (T<sub>2</sub>) to be measured.

The proton spin density (i.e. the amount of <sup>1</sup>H<sub>2</sub>O per unit of volume) can be used by itself as a marker of bulk water content in tissues (McCain and Markley, 1985; Colire et al., 1988). The <sup>1</sup>H NMR longitudinal and transverse relaxation times are also likely associated with the properties of water compartmentalized in plant organelles and interacting with macromolecules. Whereas the bulk water gives rise to a monoexponential decay of the magnetization characterized by a single time constant (T<sub>1</sub> or T<sub>2</sub>), water compartmentalized in heterogeneous systems, such as plant tissues, gives rise to multiexponential decays characterized by multiple time constants (T<sub>1,i</sub>, T<sub>2,i</sub>, where i = 1, ..., n). Water in chloroplasts, vacuoles, cytoplasm, cell walls, and extracellular spaces of leaves is expected to decay with different relaxation times. However, water molecules in different compartments may not be tightly

<sup>1</sup> This work was supported by the European Commission project ACCENT, the European Science Foundation program VOCBAS, and the Scientific Committee of the Presidential Estate of Castelporziano.

<sup>2</sup> This article is dedicated to Prof. Annalaura Segre, in memory.

\* Corresponding author; e-mail francesco.loreto@ibaf.cnr.it.

The author responsible for distribution of materials integral to the findings presented in this article in accordance with the policy described in the Instructions for Authors ([www.plantphysiol.org](http://www.plantphysiol.org)) is: Francesco Loreto ([francesco.loreto@ibaf.cnr.it](mailto:francesco.loreto@ibaf.cnr.it)).

[C] Some figures in this article are displayed in color online but in black and white in the print edition.

[W] The online version of this article contains Web-only data.

[OA] Open Access articles can be viewed online without a subscription.

[www.plantphysiol.org/cgi/doi/10.1104/pp.108.128884](http://www.plantphysiol.org/cgi/doi/10.1104/pp.108.128884)

bound, and the mixing of water from different sources may make assigning relaxation times to particular compartments less clear. The extent of averaging depends on the exchange rates from different intercellular sources, on the intrinsic relaxation times, and on cell morphology (Snaar and Van As, 1992). The effect of the exchange of water molecules usually affects  $T_1$  more than  $T_2$ . In fact, differences in  $T_1$  are rather small and are often not useful to identify water sources inside leaf mesophyll. Differences in  $T_2$  are more pronounced, as water exchange over membranes only results in a partial averaging, which depends on the size of the compartments and on the membrane water permeability (Van As, 2007). As a consequence, in plant tissue,  $T_2$  measurements usually yield more detailed information on the partitioning of water than  $T_1$  measurements (Snaar and Van As, 1992).

In ivy bark tissues (Stout et al., 1978) and in wilting leaves (Colire et al., 1988), extracellular and intracellular water have been associated with long and short  $T_2$ , respectively. Water bound in chloroplasts and vacuoles of plant cells shows even longer  $T_2$  values (Snaar and Van As, 1992; Sainis and Srinivasan, 1993). However, the interpretation of relaxation parameters in terms of domain size or of proxy properties of the various water fractions remains difficult. For example, heterogeneities of sizes and structures of cells and cellular organelles (McCain et al., 1988; Snaar and Van As, 1992; Veres et al., 1993) or binding to macromolecules at organelle level, and especially to osmolytes that may be formed under stress conditions (Walter et al., 1989; Maheswari et al., 1999; van der Weerd et al., 2002), may considerably affect NMR signal and relaxation time.

Whereas many of the commonly used measurements of water content of plant tissues are destructive (e.g. water potential or relative water content [RWC]), the NMR technique is not invasive, an important feature allowing us to sample the same material throughout a sequence of stress or dependent on its ontological status. Portable NMR instruments, with low-field magnets, have been designed such that the investigations made possible by NMR relaxation technology can now be extended to field conditions (Raich and Blümer, 2004). Van As et al. (1994) applied a purposely built low-field portable  $^1\text{H}$  NMR instrument to provide information on plant water relations on whole plants in situ. They demonstrated that low-field NMR magnets can monitor water content and water flux in plants grown in climate rooms and in greenhouses. In some portable NMR instruments, the magnetic field is applied to the sample from one side only (Eidmann et al., 1996; Blümich et al., 1998; Chang et al., 2006). This development allows easy transport of the instrumentation for in situ measurements, a very valuable advantage for plant science. Even if the magnetic field penetrating the object is rather inhomogeneous, this instrument has provided useful information in many fields of application, such as soft matter, food, biological tissue, and porous materials (Zimmer et al., 1998; Hailu et al., 2002; Sharma et al., 2003; Proietti et al., 2004, 2006, 2007).

In this article, we report the results obtained using a portable, noninvasive unilateral NMR instrument in field conditions to detect the water status of different plants. Leaves of potted herbaceous and agroforestry plants, and leaves of vegetation naturally growing in the field in Mediterranean conditions, composed principally of sclerophyllous evergreen plants and enduring a spring to summer drought stress, were used. We specifically aimed at investigating (1) whether leaf water content (as indicated by destructive assays such as RWC and pressure/volume relationships) and water loss through transpiration can be detected by changes of the NMR signal, and (2) whether the physiological state of a leaf under a developing stress (as also shown by indicators of membrane degradation) is associated with changes of the  $T_2$ .

## RESULTS

### Dehydration and Rapidly Developing Water or Osmotic Stress

In the first experiment, leaves of corn (*Zea mays*) were subjected to a fast-developing drought stress after

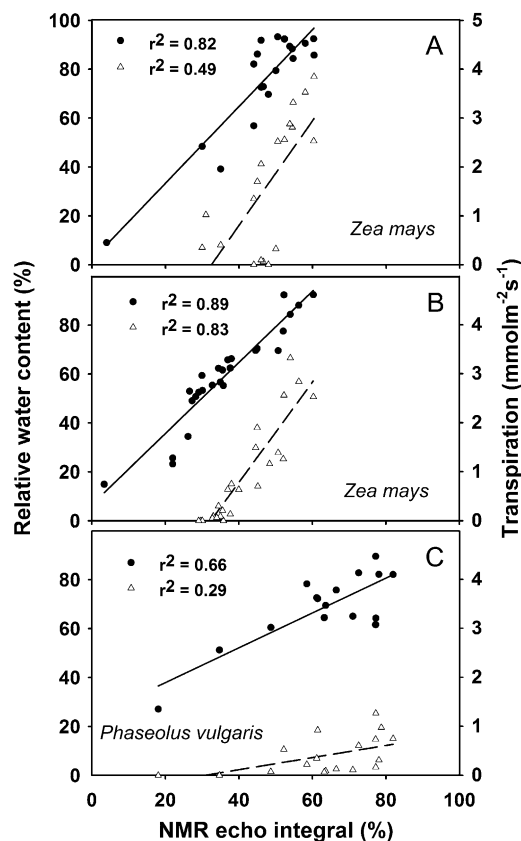


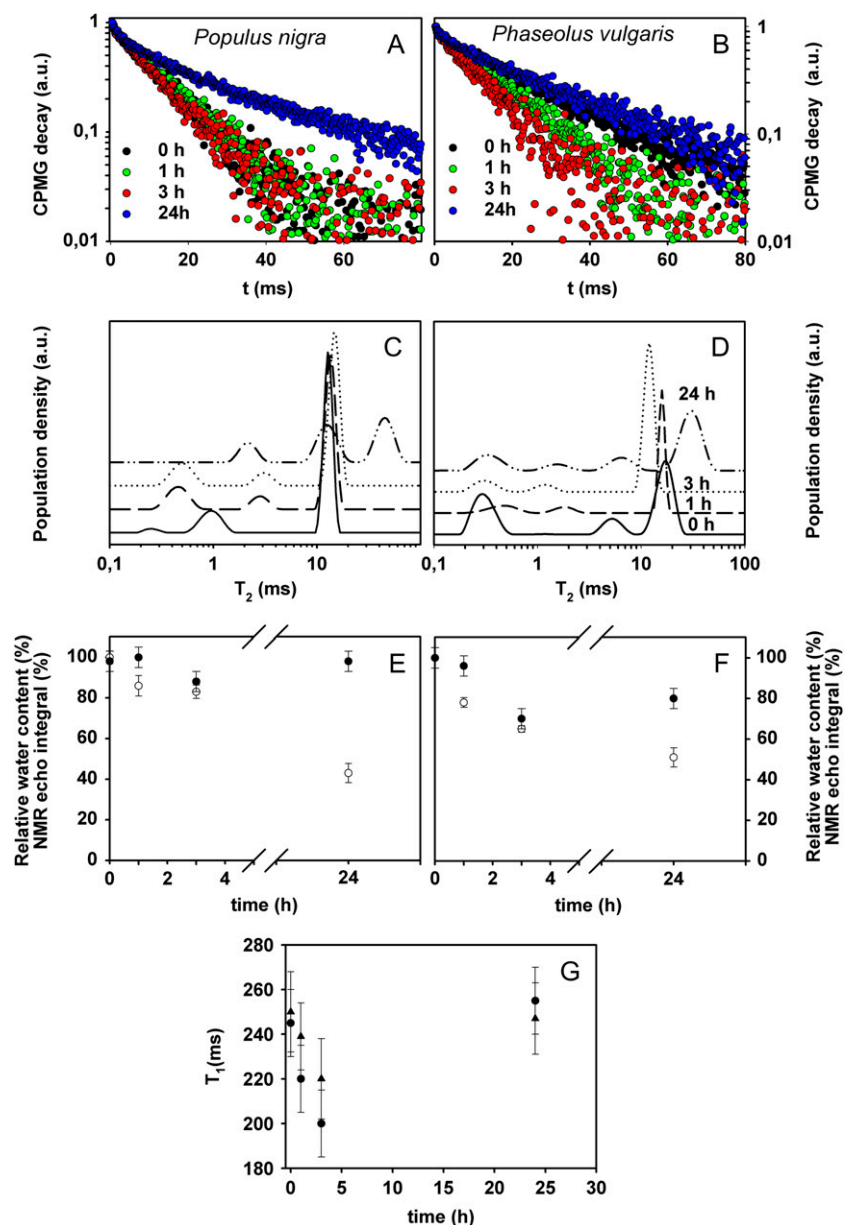
**Figure 1.** Relationship between NMR echo integral and RWC (black circles) and transpiration (white triangles) in leaves of corn plants subjected to drought stress by withholding irrigation (A) or rapidly dehydrated by cutting them from the main stem (B) and in bean leaves also rapidly dehydrated (C). Each data point represents a measurement on a different leaf. Best fits and linear regressions were calculated with Sigma Plot 9.0 software.

stopping the irrigation of the entire plants (Fig. 1A) or to a very rapid dehydration (3–5 h) after cutting the leaf from the main stem (Fig. 1B). In both cases, the reduction of RWC was clearly associated with a reduction of the integral of the NMR echo signal. More interestingly, a very good association was also found between the integral of the NMR echo signal and the transpiration rate, a nondestructive measurement of the water lost by the plant mainly through stomatal opening. RWC and transpiration were also associated with the NMR signal in bean (*Phaseolus vulgaris*) leaves rapidly dehydrated after cutting them from the plant (Fig. 1C).

Measurements of  $T_2$  and  $T_1$  were performed by applying the CPMG (for Carr-Purcell-Meiboom-Gill) sequence on leaves of black poplar (*Populus nigra*) and bean undergoing dehydration for 24 h after being cut

from the plant. In Figure 2, A and B, the CPMG decays of these leaves are reported in a semilogarithmic scale. A shortening of the decay was observed during the first 3 h of stress, whereas a longer decay was observed in all leaves after 24 h of dehydration (Fig. 2, A and B). To better visualize this trend, data were inverted by obtaining the distribution of  $T_2$  (Fig. 2, C and D). This representation is particularly suitable in the case of heterogeneous systems showing multiexponential relaxation decays. In this representation, the maxima (peaks) of the distribution are centered at the corresponding most probable  $T_2$  values, while peak areas correspond to the populations of the  $T_2$  components. During the first 3 h after the cutting, the three leaves showed at least two significant peaks, the first one in the 0.2- to 1.2-ms range, and the second one centered at

**Figure 2.** CPMG decays reported in a semilogarithmic scale and the corresponding  $T_2$  distributions measured in black poplar (A and C) and bean (B and D) leaves at time 0 and after 1, 3, and 24 h after cutting the leaves from the plants. The time course of RWC (white symbols) and NMR echo integral (black symbols) in black poplar (E) and bean (F) is also shown. NMR echo integrals were normalized to the highest value to make equal (=100) NMR and RWC values before dehydration. Finally, G shows  $T_1$  values of black poplar (circles) and bean (triangles) leaves during the dehydration time. Means  $\pm$  SE are shown ( $n = 3$ ). a.u., Arbitrary units. [See online article for color version of this figure.]



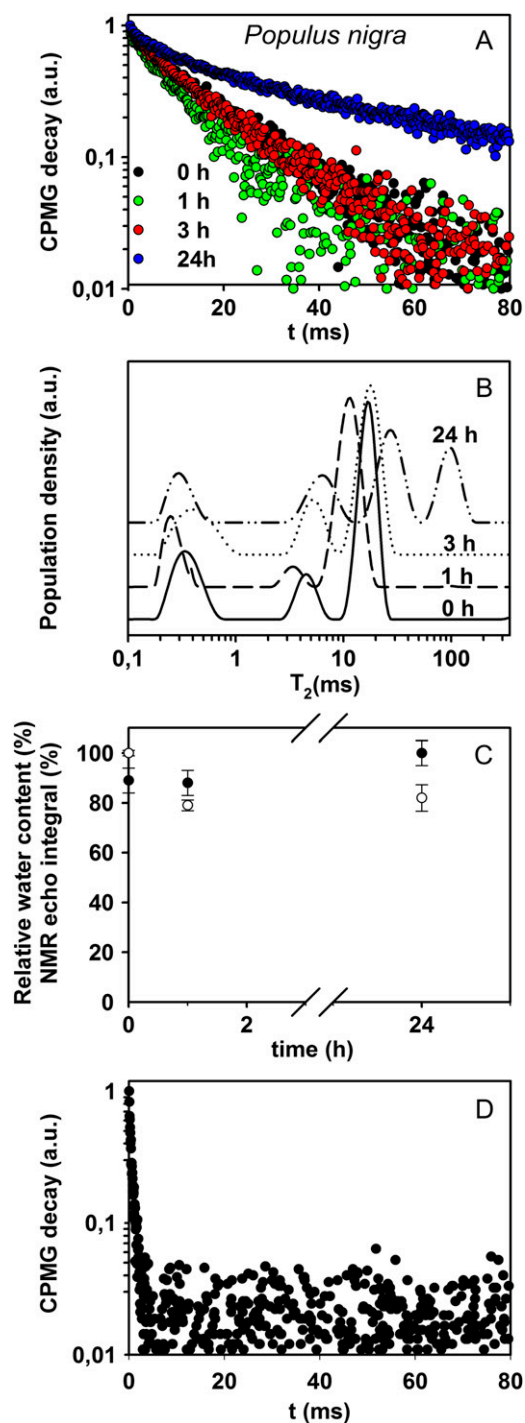


**Figure 3.** A and B, CPMG decays reported in a semilogarithmic scale (A) and  $T_2$  distributions (B) measured on black poplar leaves subjected to an osmotic stress by feeding a 50% PEG aqueous solution through the petiole of a leaf before PEG application (time 0) and after 1, 3, and 24 h. C and D, Time course of RWC (white symbols) and NMR echo integral (black symbols) in black poplar leaves before PEG application (time 0) and 1, 3, and 24 h after the treatment (C) and CPMG decay of a wilted leaf (D). NMR echo integrals were normalized to the highest value to make equal (=100) NMR and RWC values before the osmotic stress. Means  $\pm$  SE are shown ( $n = 3$ ). a.u., Arbitrary units. [See online article for color version of this figure.]

about 10 ms. In all leaves, after 24 h of dehydration, a third peak centered at about 40 ms appeared.

The results of  $T_1$  measurements performed on the same leaves of poplar and bean during the 24-h-long dehydration period are shown in Figure 2G. Although the effects of the water compartmentalization on  $T_1$  measurements are generally less pronounced than they are on  $T_2$  measurements (Snaar and Van As, 1992), due to a different averaging over the compartments, a clear reduction of  $T_1$  values was also found during the first 3 h after cutting, whereas, similar to  $T_2$ , an increase of the  $T_1$  value was recorded after 24 h of dehydration. In both poplar and bean, the NMR signal integral decreased together with RWC from 3 h after starting the dehydration treatment. However, measurements after 24 h revealed that the NMR signal integral, and the longer CPMG decay, did not match the expected further reduction of RWC in wilting leaves (Fig. 2, E and F). CPMG experiments were performed several times on different leaves, and the same behavior of the CPMG decays was observed (Supplemental Fig. S1).

A second experiment was run on poplar leaves undergoing an osmotic stress as rapid as the dehydra-

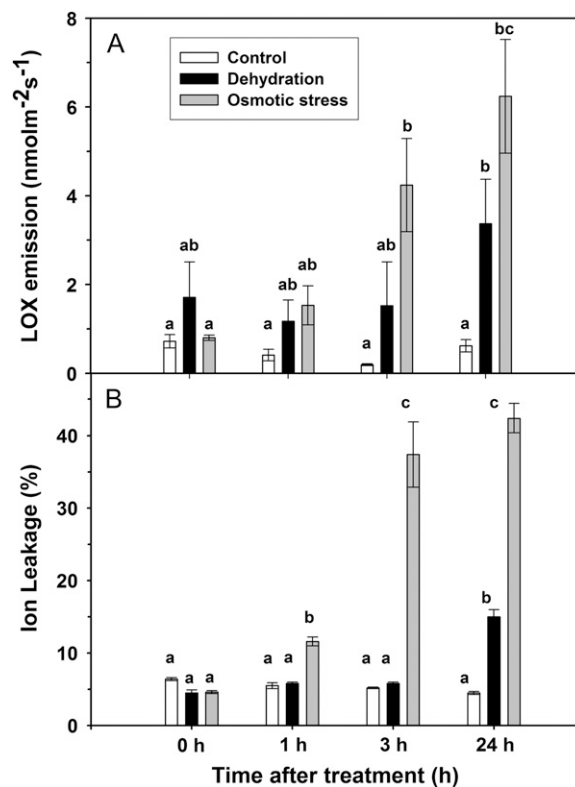


**Figure 4.** Time course of the emission of LOX products (A) and ion leakage (B) in black poplar leaves maintained under fully hydrated conditions (control; white bars) or undergoing a dehydration stress after being cut from the main stem (black bars) or an osmotic stress after being fed with a 50% PEG aqueous solution (gray bars). Bars represent means  $\pm$  SE ( $n = 3$ ), and differences between means of the same treatment over the time course of the experiment were separated by ANOVA and Tukey's test. Differences at  $P < 0.01$  and 0.10 are represented by different single and double letters, respectively.

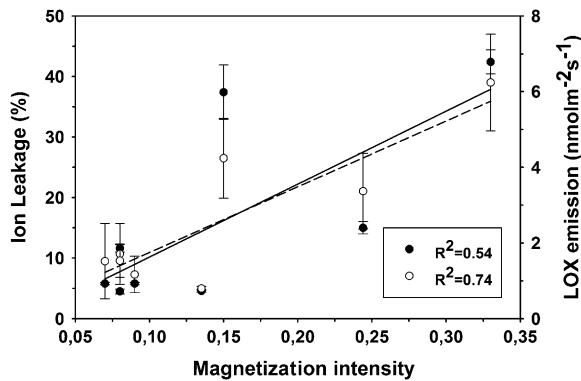


**Figure 5.** Plot of the magnetization intensity calculated at a time of 40 ms on the best fit of CPMG decays and of LOX product emissions (black circles) and of ion leakage (white circles) in control leaves of black poplar and in leaves exposed to dehydration or to osmotic stress for up to 24 h after stress initiation. Means  $\pm$  SE ( $n = 3$ ) are shown. Best fits and linear regressions (dashed line = ion leakage, solid line = LOX products emission) were calculated with Sigma Plot 9.0 software.

tion stress. Again, early stages of the osmotic stress induced a shortening of the CPMG decay (Fig. 3A) and a decrease of NMR signal integral (Fig. 3C) similar to those reported for dehydrated leaves. Also similar to the findings of the dehydration experiment, both an increase of NMR signal integral and a longer CPMG decay were observed in leaves 24 h after the application of the osmolyte. The  $T_2$  distribution reported in Figure 3B shows three peaks centered about at 0.3, 4, and 10 ms during the first 3 h of osmotic stress. After 24 h from the osmolyte application, a new peak corresponding to a much longer  $T_2$  value (i.e. 100 ms) was present.

As the stress further proceeds, a reduction of the CPMG decay occurred until a very short decay, observed in wilted leaves (Fig. 3D), indicated that only tightly bound water contributes to the NMR signal.

Two markers of cell damage were also investigated in poplar leaves subjected to the dehydration or to the osmotic stress experiments. Both *in vivo* measurements of the emission of lipoxygenase (LOX) products formed by membrane degradation (Fig. 4A) and measurements of ion leakage from leaf discs (Fig. 4B) showed clear increases of the two parameters with the time of exposure to the stresses. The increase was particularly significant and occurred somewhat earlier in leaves exposed to the osmotic stress. During the dehydration and osmotic stress experiments, the increase of the two markers was associated with the value of the magnetization intensity calculated at a time of 40 ms on the best fit curve of the CPMG decays (i.e. to the intensity of the echo at a time of 40 ms; Fig. 5).

### Slowly Developing and Reversible Water Stress

With the following experiments, we wanted to investigate whether NMR reliably assesses water content when the water stress develops slowly and is recovered

upon rewatering. Measurements of  $T_2$  were performed on poplar leaves of potted plants that were watered with 30% of the transpired water and then again irrigated to full soil capacity. A shortening of CPMG decay was observed in the first 3 d of water stress, which was followed by a lengthening of the decay after 4 and 6 d of stress (Fig. 6A). In the corresponding  $T_2$  distribution (Fig. 6B), the long  $T_2$  component appeared and was centered at about 20 and 40 ms after 4 and 6 d of stress, respectively. After a 2-d rewatering, a shortening of the decay was again observed, which corresponded to the appearance of the long  $T_2$  component back to about 20 ms. After the 2-d-long rewatering, leaves recovered about 80% of the photosynthetic rates measured before stress occurrence ( $16 \pm 2 \mu\text{mol m}^{-2} \text{s}^{-1}$ ), while photosynthesis was almost completely suppressed at the end of the water stress period (data not shown).

It is worth noting that the CPMG trend observed in the case of the slow-developing stress is very similar to the one observed in the case of fast-developing stresses, with a slight shortening of the decay during the first period of stress and a net lengthening of the decay during the last period of stress. This lengthening corresponds to the appearance of a long  $T_2$  component in the  $T_2$  distribution, centered at about 40 ms after 6 d and 24 h of stress, respectively (Figs. 2, C and D, 3B, and 6B). The lengthening of the decay should not be attributed to leaf wilting, which is characterized by an extremely

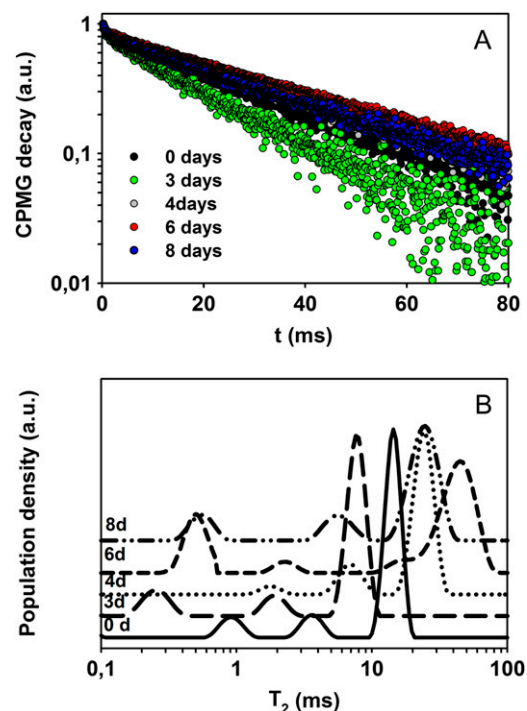


**Figure 6.** CPMG decays reported in a semilogarithmic scale (A) and  $T_2$  distributions (B) measured in black poplar during a slow dehydration of 6 d followed by a 2-d hydration (day 8 of treatment). a.u., Arbitrary units. [See online article for color version of this figure.]



short decay (Fig. 3D), but rather is typical of a reversible stress from which plants can recover.

In another experiment, destructive measurements of leaf water potential were coupled to  $T_2$  measurements on leaves of black poplar under a slow-developing water stress (20 d) followed by a 6-d recovery upon rewatering. The water stress was generated by supplying 50% of the transpired water to potted poplars. The value of the leaf water potential was correlated to the value of the NMR echo integral. As the water potential decreased, the echo integral also decreased during the stress (Fig. 7A). After the rewatering, the echo integral as well as the water potential returned to similar prestress values. When plotted together, a clear correlation between the two parameters was observed (Fig. 7B).

Finally, we performed some field measurements on the natural Mediterranean vegetation to expand the experimental range to plant species adapted to summer drought and to verify the potentiality of our instruments under field conditions. Measurements were carried out on rockrose (*Cistus incanus*) and holm oak

(*Quercus ilex*) plants before and after a rainfall during May. In rockrose leaves, which are characterized by high transpiration even under drought conditions, a concurrent increase of NMR echo integral and of water status parameters (RWC and transpiration) was observed after the rainfall (Fig. 8A). By contrast, in the water-saving, sclerophyllous leaves of holm oak, the rainfall did not change substantially either NMR echo integral or water status indicators (Fig. 8B). In rockrose leaves, the CPMG decay was faster when the plants were drought stressed than after the rainfall (Fig. 8C). By contrast, no significant differences were observed in CPMG decays measured in holm oak leaves during the drought stress and after the rainfall (Fig. 8D). The corresponding  $T_2$  distributions of rockrose and holm oak leaves are reported in Figure 8, E and F, respectively. In the drought-stressed rockrose leaves, two distributions centered at about 0.1 and 10 ms were observed, whereas after the rainfall two new distributions centered at 4 and 40 ms were also found. In holm oak leaves, however, the same distributions of  $T_2$  were observed before and after the rainfall, but two peaks, centered at about 2 and 5 ms, that were observed in drought-stressed leaves, collapsed to just one larger peak centered at about 3.5 ms after the rainfall (Fig. 8F).

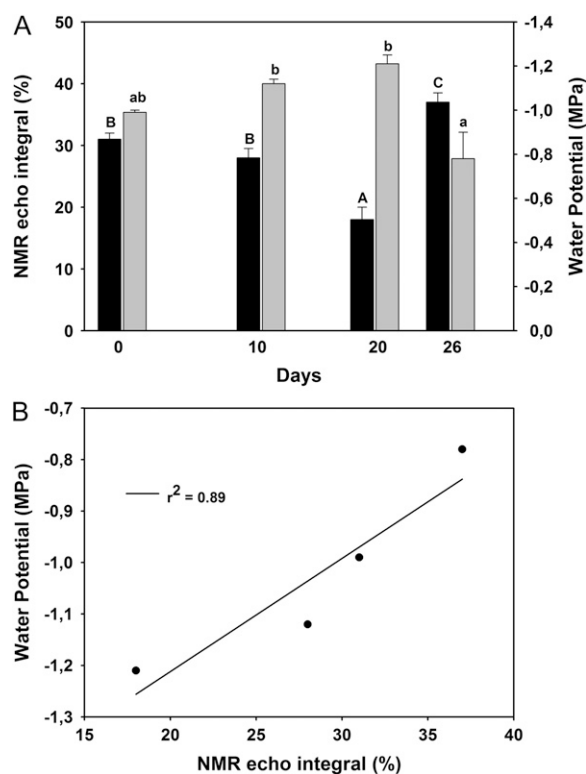
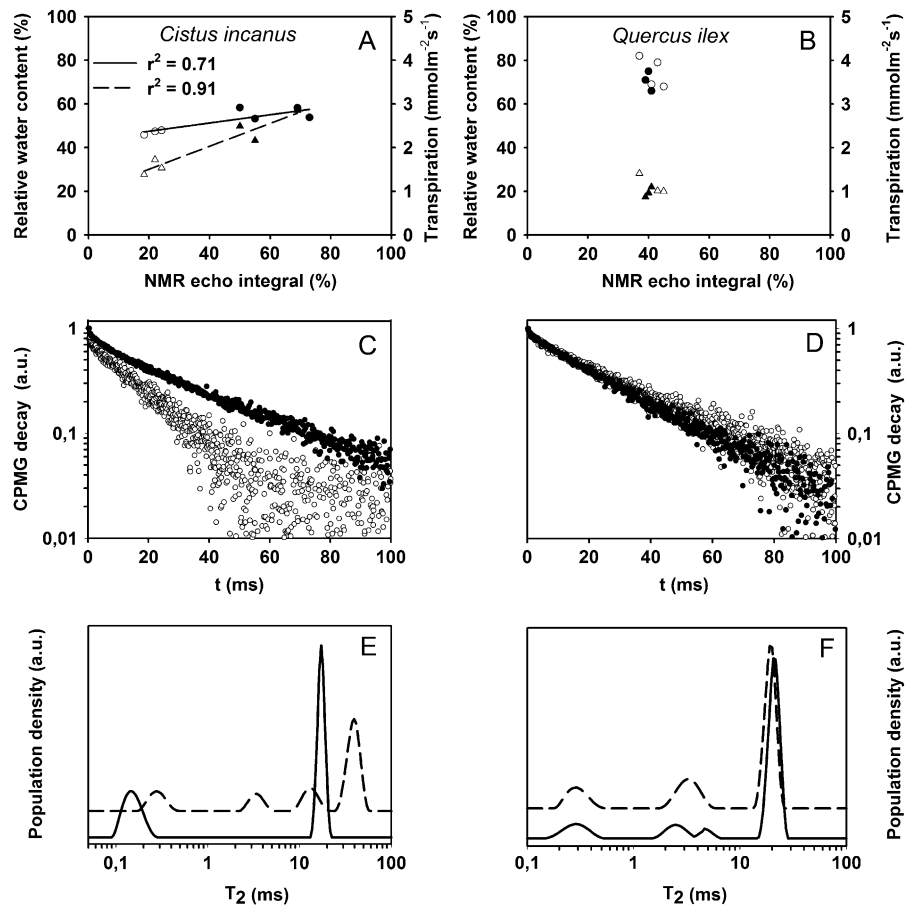


**Figure 7.** A, NMR echo integral (black bars) and leaf water potential (gray bars) during a slowly developing water stress and during recovery from stress (day 26) in black poplar leaves. Means  $\pm$  SE ( $n = 3$ ) are shown. Differences between means of NMR echo integral and leaf water potential over the time course of the experiment were separated by ANOVA and Tukey's test. Differences at  $P < 0.01$  and  $0.10$  are represented by different single and double letters, respectively. B, The two indices are plotted against each other to better illustrate the relationship observed during the entire experiment.

## DISCUSSION

$^1\text{H}$  NMR measurements carried out with a unilateral instrument operating at low magnetic field are indeed a good proxy for leaf water status, confirming results previously obtained with laboratory instrumentation at high magnetic fields (Colire et al., 1988; Reinders et al., 1988) and with a different portable NMR instrument (Van As et al., 1994). Our experimentation on potted plants indicates that NMR signal integral is associated with the leaf water status. In unstressed conditions, a higher NMR signal integral was found in mesophyllous plants, either herbs or trees (e.g. maize or poplar) than in oak, the only sclerophyllous plant that was tested. This may be due to the different water content (fresh weight) in unstressed samples, an issue that was not investigated in this work. In stressed leaves, the relationship between NMR signal integral and leaf water status indicators was found both when the water stress was induced rapidly and when it developed slowly and was fully recovered. Interestingly, a relationship was also found between NMR signal integral and transpiration rate. This indicates that NMR measurements may effectively be used to monitor the water lost by plants through stomata and cuticle and the degree of stomatal opening. Stomatal closure may in turn limit  $\text{CO}_2$  acquisition and photosynthesis, especially in stressful conditions (Flexas et al., 2004). If these results are confirmed by a more complete and focused screening, including uncoupling of changes of transpiration and water potential, unilateral NMR technology may become a useful tool

**Figure 8.** A and B, Field measurements on natural Mediterranean vegetation. Shown is the relationship between NMR echo integral and RWC (circles) and transpiration (triangles) in leaves of rockrose (A) and holm oak (B) before (white symbols) and after (black symbols) a rainfall. C to F, CPMG decays reported in a semilogarithmic scale (C and D) and  $T_2$  distributions (E and F) measured in rockrose (C and E) and holm oak (D and F) leaves before (white symbols [C and D], solid lines [E and F]) and after (black symbols [C and D], dashed lines [E and F]) a rainfall. Each symbol represents  $n = 3$ , and the SE was below the symbol size. Best fits and linear regressions were calculated with Sigma Plot 9.0 software. a.u., Arbitrary units.



to improve irrigation practices for maximizing crop production and water saving.

The relationship between RWC and NMR signal integral was also observed in herbaceous leaves and in the leaves of the mesophyllous tree black poplar during the early induction of dehydration or osmolytic stress. However, this relationship was lost after 24 h of dehydration. This effect could be caused by shrinking of the dehydrating leaves, in turn reducing the volume of air proportionally more than the volume of water contained in the leaf. However, we did not observe significant changes in leaf geometry after 24 h of dehydration. To better investigate why RWC and NMR signal integral are not associated in heavily dehydrated leaves, the  $T_2$  was measured. Measurements of  $T_2$  may reveal different water populations in the leaf. Free, extracellular water molecules show longer  $T_2$  than water molecules bound to cellular structures and macromolecules (Walter et al., 1989).  $T_2$  relaxation may also depend on membrane permeability controlling the flux of water between compartments and from cellular structures to the extracellular apoplasm (van der Weerd et al., 2002). The observed shortening and lengthening of CPMG decays, corresponding to a decrease of  $T_2$  in leaves undergoing dehydration or osmolytic stress for a few hours and to an increase of  $T_2$  after 24 h of dehydration, may

be explained in terms of variation of membrane permeability. In particular, a decrease in  $T_2$  is observed when the membrane permeability increases. In fact, increased membrane permeability, possibly due to the activity of aquaporins, may facilitate water transport and maintain cellular expansion during the stress. On the other hand, a  $T_2$  increase may be observed if membranes become less permeable to water pools to preserve cellular water within the tissues (van der Weerd et al., 2002). Cavitation of veins could also play a role in changing the CPMG decay, but we expect that air entering the cavitated vessel pumps out the remaining water, thus contributing to a decrease of  $T_2$ .

Both the ion leakage, indicating higher permeability of membranes as a consequence of stress induced to their structures (Gupta, 1977), and the release of products of membrane lipooxygenation, indicating damage to the lipoproteic structure of the membranes (Loreto et al., 2006), increased during the dehydration and the osmotic stress, and both membrane stress markers reached their highest levels 24 h after beginning the treatment. Increasing levels of both stress markers were associated with the increase of the magnetization intensity calculated at a time of 40 ms on the best fit curve of the CPMG decays. This may indicate that a correspondence exists between the variation in membrane

permeability of some leaf cells and the denaturation of the membranes. Denatured membranes, however, should lose water more freely, which should shorten the CPMG decay. Perhaps both responses can be observed simultaneously in different cell categories of dehydrating leaves, with factors slowing membrane permeability playing a predominant role in determining the NMR signal. The net lengthening of the CPMG decay that was observed after 6 d of slow-developing water stress in poplar leaves that later recovered from the stress might also indicate a reduced permeability of water pools across membranes, in turn revealing a reduced activity of aquaporins under certain natural conditions.

The measurements conducted in a natural environment in two species with contrasting strategies with respect to water relations gave further information and confirmed some results discussed previously. A significant relationship between NMR signal integral and RWC and transpiration was obtained in rockrose, a plant species characterized by a small leaf thickness and by a water-spending strategy, that is, with a small degree of control of stomatal conductance on water flux (Correia and Catarino, 1994). In the case of sclerophyllous holm oak, the NMR signal and the two parameters monitoring leaf water status did not substantially change. In fact, sclerophyllous plants have dense and thick leaves that reduce the exchange of water and CO<sub>2</sub> with the atmosphere (Loreto et al., 1992) and are at the base of an ecological water-saving strategy (Chaves et al., 2002). Consistently, in these leaves, we detected very low and rather constant transpiration rates and low and constant NMR signal integrals as well, in comparison with those observed in herbaceous leaves and in rockrose.

Moreover, in leaves of the water-spending *Cistus*, CPMG decay of drought-stressed plant was faster than the decay observed in the same plant after the rainfall. In contrast, no significant differences were observed in CPMG decays measured in *Quercus* leaves during the drought stress and after the rainfall, confirming that in this sclerophyllous plant the cellular compartmentalization of water is maintained even during a stressful event and that mechanisms facilitating water diffusion do not play a relevant role in these plants.

The investigation of T<sub>2</sub> distributions in the leaves of natural vegetation also showed that only in *Cistus* leaves, but not in *Quercus* leaves, two more peaks appeared after the rainfall, possibly indicating a water uptake in other preferential leaf compartments. Alternatively, the new peaks might be attributed to increased release of water due to cell expansion (van der Weerd et al., 2001) or activation of water channels (van der Weerd et al., 2002).

Summarizing, these observations indicate that the unilateral NMR instrumentation is a useful tool for revealing in situ changes in the water status of leaves, for screening vegetation health and fitness in natural and cultivated conditions, and for identifying mechanistic processes as the basis of the observed response.

However, to perform correct measurements, it is important to consider that the magnetic field generated by the portable instrument is inhomogeneous. Therefore, the instrument does not allow the direct measurement of the free induction decay and the signal is always observed as an echo signal. Moreover, the inhomogeneous field is a further source of relaxation, which shortens the measured T<sub>2</sub> values. To minimize this effect, the CPMG pulse sequence must be carried out with echo time values ( $\tau$ ) values as short as possible, but T<sub>2</sub> values measured with unilateral NMR may still be shorter than those measured in a highly homogeneous field. As a rule, only CPMG decays collected using the same  $\tau$  value should be compared. Finally, it is important to consider that the sensitivity of the unilateral NMR probe head strongly depends on the distance between the radio frequency coil and the leaf and that the probe head should be selected to give the maximum signal intensity at a distance corresponding to the thickness of the investigated leaves.

## MATERIALS AND METHODS

### Plant Material and Growth Conditions

#### Potted Plants

Plants of bean (*Phaseolus vulgaris*) and corn (*Zea mays*) were grown from seeds individually planted in 5-dm<sup>3</sup> pots. Black poplar (*Populus nigra*) saplings were propagated from physiologically mature trees of a clonal provenance in Italy. After rooting, the cuttings were potted in 5-dm<sup>3</sup> pots. All of the pots were filled with commercial soil. All plants were grown in a climatic chamber (Sanyo Gallenkamp) under controlled conditions, namely a light intensity of 700 to 800  $\mu\text{mol m}^{-2} \text{s}^{-1}$  for 16 h daily, day/night temperatures of 25°C/22°C  $\pm$  2°C, and day/night relative humidity of 50%/60%. Plants were regularly watered to keep the pots at full water capacity and fertilized with Hoagland solution once per week in order to supply mineral nutrients at free access rate. Experiments started 1 month after growing plants under the above-specified conditions.

#### Natural Vegetation

Plants of *Cistus incanus* (rockrose) and *Quercus ilex* (holm oak) naturally growing on a sand dune in the protected area of the Presidential Estate of Castelporziano (Rome; 41° 41' 54" N, 12° 21' 10" E) were used. These measurements were performed in May during a field campaign.

### Experimental Conditions

Plants were subjected to treatments to manipulate the water content of the leaves. Only fully developed and healthy leaves were used. Corn and poplar plants were exposed to a slow-developing drought by stopping irrigation of the pots. Corn, poplar, and bean leaves were also quickly dehydrated by cutting them off the plants. Cut poplar leaves maintained with the petiole in a beaker with water to allow for optimal water conditions were osmotically stressed by adding polyethylene glycol (PEG; Aldrich) to the water to obtain a 50% PEG aqueous solution.

Field measurements on natural vegetation were carried out on leaves that were naturally water stressed by a 1-month-long drought period during May and were repeated on the same leaves on the day after an 8-mm rainfall.

### NMR Measurements

All measurements were performed at 18.153 MHz with a commercial unilateral NMR instrument (Eureka project  $\Sigma$ 12214) from Bruker Biospin Italy. The probe head is made of a U-shaped magnet assembly with two permanent



magnets mounted on an iron yoke and includes a radio frequency resonator properly designed for avoiding detuning effects. The maximum echo signal, corresponding to a  $\pi/2$  pulse, was obtained with a pulse width of 3  $\mu\text{s}$ , and the dead time was 13  $\mu\text{s}$ .

Measurements were carried out nondestructively on single leaves attached to the plants or detached from the plants according to the different experimental protocols. The sampled leaf was positioned in contact with the probe head and kept immobile with a piece of glass free of any  $^1\text{H}$  NMR signal. Each measurement was carried out within few minutes under experimental conditions that perturbed the leaf functionality only minimally, as indicated by concurrent physiological measurements of water relations.

Since in a nonhomogeneous magnetic field the NMR signal decays very quickly, the NMR signal can be recovered stroboscopically (Blümich et al., 2003). Therefore, the signal intensity or integral is actually the intensity or integral of the signal resulting after applying a single Hahn echo sequence (Fukushima and Roeder, 1981).

The total water content in the leaf was estimated by performing single Hahn echo measurements with an echo time of 50  $\mu\text{s}$ . An echo time of 50  $\mu\text{s}$  was purposely chosen for suppressing the signal of the solid component of the leaves (cellulose, lignin). In fact, the average  $T_2$  value of the solid component is about 20 to 30  $\mu\text{s}$ . In all single Hahn echo experiments, the number of scans was fixed to 512. A recycle delay of 2 s was used. As a result of Hahn echo experiments, the intensity, the integral, the average noise, and the signal-to-noise ratio were obtained directly from the software. It is worth noting that the intensity and the integral of the Hahn echo, in all cases, showed the same trend. However, in the figures, the integral of the NMR echo signal was reported as a percentage with respect to the free water integral value. Real data were always used in the processing of the experimental data.

The values of the magnetization intensity reported in Figure 5 were calculated at a time of 40 ms on the best fit curve of the CPMG decays; in fact, at this time, the decays are well distinguishable and the corresponding magnetization values are not affected by the noise.

Transverse  $T_2$  values were measured with the CPMG sequence following the procedure published previously (Carr and Purcell, 1954; Meiboom and Gill, 1958), and 2,048 echoes were recorded using a delay  $2\tau$  of 50  $\mu\text{s}$  ( $\tau = 25 \mu\text{s}$ ). A recycle delay of 2 s was used. In all CPMG experiments, the number of scans was fixed at 1,024. Real data were always used in the processing of the experimental data.

The echo decays, obtained by applying the CPMG sequence, were treated as multiexponential decays as follows:

$$Y = C_0 + \sum_i W_i \exp\left[-\frac{t}{T_{2i}}\right] \quad (1)$$

where  $i$  is the number of components,  $C_0$  is the offset value,  $W_i$  is the weight of the  $i$  component, and  $T_{2i}$  is the transversal relaxation time of the  $i$  component.

A regularized inverse Laplace transformation (Press et al., 1994) was applied to the echo decay obtained by applying a CPMG sequence. After the transformation, the experimental  $T_2$  decays were represented as a distribution of  $T_2$  relaxation times. Distributions were obtained using a software implemented within the Matlab (MathWorks) framework.

$T_1$  values were measured with the aperiodic saturation recovery sequence (Farrar and Becker, 1971), and 128 blocks were collected. As in all cases, the maximum  $T_1$  value measured was always shorter than 300 ms, and a recycle delay of 2 s was used in all experiments. In all  $T_1$  experiments, the number of scans was fixed at 256. Real data were always used in the processing of the experimental data.

## Leaf Water Measurements

Transpiration was measured with a portable photosynthetic system (LI 6400; Li-Cor) immediately before NMR measurements and on the same leaf portion. The leaf was clamped in a gas-exchange cuvette and maintained under environmental conditions set to reproduce the growth conditions (leaf temperature = 25°C, incident light intensity = 800  $\mu\text{mol m}^{-2} \text{s}^{-1}$ , relative humidity = 40%,  $\text{CO}_2$  concentration in air = 370  $\mu\text{mol mol}^{-1}$ ). The leaf was exposed to a 0.3 L  $\text{min}^{-1}$  air flow, and the difference of water vapor in the air before and after the leaf was used to calculate leaf transpiration and stomatal conductance (von Caemmerer and Farquhar, 1981).

The RWC of a leaf is defined as follows:

$$\text{RWC} (\%) = 100 (W_f - W_d) / (W_f - W_d)$$

where  $W_f$  is fresh leaf weight,  $W_t$  is turgid leaf weight, and  $W_d$  is dry leaf weight. To measure RWC in the leaves near those used for NMR and transpiration measurements, portions (1  $\text{cm}^2$ ) of the same leaf were taken at different stages during treatments and the  $W_f$  was immediately weighed. The same samples were then floated in water for 12 h to measure the  $W_t$  and then oven dried at 80°C overnight to measure the  $W_d$ .

To measure leaf water potential, fully expanded black poplar leaves were detached from different plants during the water stress treatment. Leaves were weighed and placed in a pressure chamber (Soil Moisture Equipment Corp.) to determine the pressure at which water is exuded from the petiole (Scholander et al., 1965).

## Measurements of Cell Damage

### Ion Leakage Measurements

Solute leakage has been used in the past to assess membrane integrity in response to environmental stresses such as chilling (Leopold and Musgrave, 1979), freezing (Palta et al., 1977), and dehydration (Gupta, 1977). Poplar leaf discs (1  $\text{cm}^2$ ) were collected on leaves subjected to dehydration or fed with PEG, as described above, after NMR measurements. The leaf samples were placed in 5-mL vials with 2 mL of deionized water and were kept in the dark at 4°C. After 1 h, the electrical conductance of the leachate was measured using a conductivity meter (Amber Science 1051). The relative amount of leakage is expressed as a percentage of the maximum conductance measured after autoclaving the sample at 110°C for 10 min.

### LOX Product Emission Measurements

Poplar leaves were enclosed in a 0.5-L gas-exchange cuvette (Walz) and exposed to the above-specified rapid dehydration or osmotic stress. Leaves were maintained under a 1 L  $\text{min}^{-1}$  flow of clean synthetic air (80%  $\text{N}_2$ , 20%  $\text{O}_2$ , and 370  $\mu\text{mol mol}^{-1}$   $\text{CO}_2$ ) while thermostatted at 25°C and illuminated with 800  $\mu\text{mol m}^{-2} \text{s}^{-1}$  white light with the system described by Loreto et al. (1994) for  $\text{CO}_2$ - and water-exchange measurements. However, part of the air leaving the cuvette was redirected through a Teflon valve to a proton transfer reaction mass spectrometer (Ionicon) for measurements of released volatile organic compounds (Lindinger et al., 1998). We focused the attention on the release of products of volatile organic compounds produced by the octadecanoid pathway of membrane lipoxidation under stress conditions (LOX products). As demonstrated previously (Beauchamp et al., 2005), the total amount of LOX products emitted can be estimated by summing the signals obtained for the molecular ion and the main fragment of (Z)-3-hexenal (mass 99 and 81) and (Z)-3-hexenal + (E)-2-hexenal (mass 101 and 83). In order to increase proton transfer reaction mass spectrometry sensitivity for these LOX compounds, all of the analyses were performed at low ionization energy (approximately 90 Td) using mass 37 ( $\text{H}_2\text{O}^+\text{H}_3\text{O}^+$ ) as a primary ion source. For each LOX compound, the instrument was calibrated daily with gaseous standard.

## Statistics

All measurements were obtained on at least three different leaves of different plants. Results from all sampled leaves are shown for measurements of NMR signal integral, while  $T_2$  is reported for a single leaf, with more replications shown in Supplemental Figure S1. Linear regression coefficients and means  $\pm$  SE were calculated by Sigma Plot 9.0 (Systat Software). Means of the indicators of cell damage, and the NMR echo integral in relation to leaf water potential, were separated in an ANOVA scheme by a Tukey's test. Differences at  $P < 0.01$  and 0.10 are represented in the figures by different single and double letters, respectively.

## Supplemental Data

The following materials are available in the online version of this article.

**Supplemental Figure S1.** CPMG decays reported in a semilogarithmic scale, relative to three leaves (A–C) of black poplar and the corresponding  $T_2$  distributions (D–F).

## ACKNOWLEDGMENTS

We thank Silvano Fares, Marco Gobbino, and Sara Cozzolino for their help with laboratory and field measurements.

Received September 2, 2008; accepted February 2, 2009; published February 4, 2009.

## LITERATURE CITED

- Beauchamp J, Wisthaler A, Hansel A, Kleist E, Miebach M, Niinemets U, Schurr U, Wildt J** (2005) Ozone induced emissions of biogenic VOC from tobacco: relationships between ozone uptake and emission of LOX products. *Plant Cell Environ* **28**: 1334–1343
- Blümich B, Anferova S, Kremer K, Sharma S, Herrmann V, Segre AL** (2003) Unilateral nuclear magnetic resonance for quality control: the NMR-MOUSE. *Spectroscopy* **18**: 18–32
- Blümich B, Blümer P, Eidmann G, Guthausen A, Haken R, Schmitz U, Saito K, Zimmer G** (1998) The NMR-mouse: construction, excitation, and applications. *Magn Reson Imaging* **16**: 479–484
- Bottomley PA, Rogers HH, Foster TH** (1986) NMR imaging shows water distribution and transport in plant root systems in situ. *Proc Natl Acad Sci USA* **83**: 87–89
- Carr HY, Purcell EM** (1954) Effects of diffusion on free precession in nuclear magnetic resonance experiments. *Phys Rev* **94**: 630–638
- Chang WH, Chen JH, Hwang LP** (2006) Single-sided mobile NMR with a Halbach magnet. *Magn Reson Imaging* **24**: 1095–1102
- Chaves MM, Pereira JS, Maroco J, Rodrigues ML, Ricardo CPP, Osorio ML, Carvalho I, Faria T, Pinheiro C** (2002) How plants cope with water stress in the field? Photosynthesis and growth. *Ann Bot (Lond)* **89**: 907–916
- Colire C, Le Rumeur E, Gallier J, de Certaines J, Larher F** (1988) An assessment of proton nuclear magnetic resonance as an alternative method to describe water status of leaf tissues in wilted plants. *Plant Physiol Biochem* **26**: 767–776
- Correia OA, Catarino FM** (1994) Seasonal changes in soil-to-leaf resistance in *Cistus* sp. and *Pistacia lentiscus*. *Acta Oecol* **15**: 289–300
- Eidmann G, Savelsberg R, Blümer P, Blümich B** (1996) The NMR mouse, a mobile universal surface explorer. *J Magn Reson A* **122**: 104–109
- Farrar TC, Becker ED** (1971) Pulse and Fourier Transform NMR. Academic Press, New York
- Flexas J, Bota J, Loreto F, Cornic G, Sharkey TD** (2004) Diffusive and metabolic limitations to photosynthesis under drought and salinity in C3 plants. *Plant Biol* **6**: 269–279
- Fukushima E, Roeder SBW** (1981) Experimental Pulse NMR: A Nuts and Bolts Approach. Addison-Wesley Publishing, Boston
- Gupta RK** (1977) A study of photosynthesis and leakage of solutes in relation to desiccation effects in bryophytes. *Can J Bot* **55**: 1186–1194
- Hailu K, Fechete R, Demco DE, Blümich B** (2002) Segmental anisotropy in strained elastomers detected with a portable NMR scanner. *Solid State Nucl Magn Reson* **22**: 327–343
- Leopold AC, Musgrave ME** (1979) Respiratory changes with chilling injury of soybeans. *Plant Physiol* **64**: 702–705
- Lindinger W, Hansel A, Jordan A** (1998) Proton-transfer-reaction mass spectrometry (PTR-MS): on-line monitoring of volatile organic compounds at pptv levels. *Chem Soc Rev* **27**: 347–354
- Loreto F, Barta C, Brilli F, Noguez I** (2006) On the induction of volatile organic compound emissions by plants as consequence of wounding or fluctuations of light and temperature. *Plant Cell Environ* **29**: 1820–1828
- Loreto F, Di Marco G, Tricoli D, Sharkey TD** (1994) Measurements of mesophyll conductance, photosynthetic electron transport and alternative electron sinks of field grown wheat leaves. *Photosynth Res* **41**: 397–403
- Loreto F, Harley PC, Di Marco G, Sharkey TD** (1992) Estimation of the mesophyll conductance to CO<sub>2</sub> flux by three different methods. *Plant Physiol* **98**: 1437–1443
- Maheswari M, Joshi DK, Saha R, Nagarajan S, Gambhir PN** (1999) Transverse relaxation time of leaf water protons and membrane injury in wheat (*Triticum aestivum* L.) in response to high temperature. *Ann Bot (Lond)* **84**: 741–745
- Manz B, Mueller K, Kucera B, Volke F, Leubner-Metger G** (2005) Water uptake and distribution in germinating tobacco seeds investigated in vivo by nuclear magnetic resonance imaging. *Plant Physiol* **138**: 1538–1551
- Meiboom S, Gill D** (1958) Modified spin-echo method for measuring nuclear relaxation times. *Rev Sci Instrum* **29**: 688–691
- McCain DC, Croxdale J, Markley JL** (1988) Water is allocated differently in sun and shade leaves. *Plant Physiol* **86**: 16–18
- McCain DC, Markley JL** (1985) A theory and a model for interpreting the proton nuclear magnetic resonance spectra of water in plant species. *Biophys J* **48**: 687–694
- Palta JP, Levitt J, Stadelmann EJ** (1977) Freezing injury in onion bulb cells. I. Evaluation of the conductivity method and analysis of ion and sugar efflux from injured cells. *Plant Physiol* **60**: 393–397
- Press WH, Teukolsky WT, Vetterling BP, Flannery BP** (1994) Numerical Recipes in Chemistry. Cambridge University Press, Cambridge, UK
- Proietti N, Capitani D, Cozzolino S, Valentini M, Pedemonte E, Trinci E, Vicini S, Segre AL** (2006) In situ and frontal polymerization for the consolidation of porous stones: a unilateral NMR and magnetic resonance imaging study. *J Phys Chem B* **110**: 23719–23728
- Proietti N, Capitani D, Pedemonte E, Blümich B, Segre A** (2004) Monitoring degradation in paper: non-invasive analysis by unilateral NMR. Part II. *J Magn Reson* **170**: 113–120
- Proietti N, Capitani D, Rossi E, Cozzolino S, Segre AL** (2007) Unilateral NMR study of a XVI century wall painted. *J Magn Reson* **186**: 311–318
- Raich H, Blümer P** (2004) Design and construction of a dipolar Halbach array with a homogeneous field from identical bar magnets. *NMR Mandhalas Conc Magn Reson B: Magn Reson Eng* **23B**: 16–25
- Ratcliffe RG, Shachar-Hill Y** (2001) Probing plant metabolism with NMR. *Annu Rev Plant Physiol Plant Mol Biol* **52**: 499–526
- Reinders JEA, Van As H, Schaafsma TJ, de Jager PA, Sheriff DW** (1988) Water balance in *Cucumis* plants, measured by nuclear magnetic resonance. *J Exp Bot* **39**: 1199–1210
- Sainis JK, Srinivasan VT** (1993) Effect of the state of water as studied by pulsed NMR on the function of Rubisco in a multienzyme complex. *J Plant Physiol* **142**: 564–568
- Scheenen TWJ, van Dusschoten D, de Jager PA, Van As H** (2000) Quantification of water transport in plants with NMR imaging. *J Exp Bot* **51**: 1751–1759
- Scholander PF, Hammel HT, Bradstreet ED, Hemmingsen EA** (1965) Sap pressure in vascular plants. *Science* **148**: 339–346
- Sharma S, Casanova F, Wache W, Segre A, Blümich B** (2003) Analysis of historical porous building materials by the NMR-MOUSE. *Magn Reson Imaging* **21**: 249–255
- Snaar JEM, Van As H** (1992) Probing water compartment and membrane permeability in plant cells by proton NMR relaxation measurements. *Biophys J* **63**: 1654–1658
- Stout DG, Steponkus PL, Cotts RM** (1978) Nuclear magnetic resonance relaxation times and plasmalemma water exchange in ivy bark. *Plant Physiol* **62**: 636–641
- Van As H** (2007) Intact plant MRI for the study of cell water relations, membrane permeability, cell-to-cell and long-distance water transport. *J Exp Bot* **58**: 743–756
- Van As H, Reinders JEA, de Jager PA, van der Sanden PACM, Schaafsma TJ** (1994) In situ plant water-balance studies using a portable NMR spectrometer. *J Exp Bot* **45**: 61–67
- van der Weerd L, Claessens MMAE, Efde C, Van As H** (2002) Nuclear magnetic resonance imaging of membrane permeability changes in plants during osmotic stress. *Plant Cell Environ* **25**: 1538–1549
- van der Weerd L, Claessens MMAE, Ruttink T, Vergeldt FJ, Schaafsma TJ, Van As H** (2001) Quantitative NMR microscopy of osmotic stress responses in maize and pearl millet. *J Exp Bot* **52**: 2333–2343
- Veres JS, Cofer GP, Johnson GA** (1993) Magnetic resonance imaging of leaves. *New Phytol* **123**: 769–774
- Verpoorte R, Choi YH, Kim HK** (2007) NMR-based metabolomics at work in phytochemistry. *Phytochem Rev* **6**: 3–14
- von Caemmerer S, Farquhar GD** (1981) Some relationships between the biochemistry of photosynthesis and the gas exchange of leaves. *Planta* **153**: 376–387
- Walter L, Balling A, Zimmermann U, Haase A, Kuhn W** (1989) Nuclear-magnetic-resonance imaging of leaves of *Mesembryanthemum crystallinum* L. plants grown at high salinity. *Planta* **178**: 524–530
- Zimmer G, Guthausen A, Blümich B** (1998) Characterization of cross-link density in technical elastomers by the NMR-MOUSE. *Solid State Nucl Magn Reson* **13**: 183–190

## Supplementary material

**Figure 1S.** CPMG decays reported in a semi-logarithmic scale, relative to three leaves (a, b and c), of *Populus nigra* and the corresponding  $T_2$  distributions (d, e and f).

